

Self-consistent kinetic model of the cathode fall of a glow discharge

T. J. Sommerer

Department of Physics, University of Wisconsin, Madison, Wisconsin 53706

W. N. G. Hitchon

Department of Electrical and Computer Engineering, University of Wisconsin, Madison, Wisconsin 53706

J. E. Lawler

Department of Physics, University of Wisconsin, Madison, Wisconsin 53706

(Received 16 November 1988; revised manuscript received 27 January 1989)

The electrons in the cathode-fall (CF) region of a helium dc glow discharge have been modeled at the kinetic level with a self-consistent electric field using a "convective-scheme" (CS) (propagator or Green's-function) solution method. The CS is both straightforward to implement and numerically efficient. CS electron calculations using one spatial and two velocity variables are shown to match Monte Carlo simulations of swarms in uniform E/N and in the CF. The CS predictions are also shown to match experimental swarm results. A self-consistent CF solution is obtained through a slow relaxation of the electric field to that indicated by Poisson's equation. The electric field configuration as predicted by the CS agrees well with optogalvanic measurements. The discussion emphasizes both the physical nature of, and the difficulties associated with, a self-consistent-field calculation.

I. INTRODUCTION

Interest in modeling glow-discharge properties has increased with the application of glow discharges to plasma processing. Understanding of the cathode fall (CF) is crucial to a global understanding of the discharge, as this region largely determines the stability of the discharge and the details of many plasma processes.

Efforts to model the CF are hampered by the lack of hydrodynamic equilibrium in the region due to the relatively strong electric field gradients and the presence of the cathode, which both absorbs and emits particles. Nonhydrodynamic conditions call into question the use of ionization and diffusion coefficients,¹ which are measured in swarm experiments at very low current densities and in spatially invariant electric fields. The absolute electron number density scales out of the solution when an *a priori* electric field is imposed and the behavior of other charged species is ignored, as is done in many Monte Carlo simulations. In contrast, a fully kinetic solution of the electron behavior in the cathode-fall region eliminates the use of empirical coefficients, and a self-consistent-field calculation couples the behavior of all charged species into the problem through Poisson's equation.

An overall approach to a self-consistent model of the CF region has been described in a previous paper.² There, a simple distribution function was assumed, and two moment equations, together with Poisson's equation, were integrated to demonstrate the validity of the proposed framework. This work implements a kinetic description of the electrons within a similar framework. The kinetic description is based on the convective scheme (CS), which is introduced to gaseous electronics in this paper.

This paper will begin with a brief discussion of several

methods that have been used to model weakly ionized plasmas. In this way the CS will be couched in terms of more familiar approaches. The strengths and weaknesses of these methods will be discussed, as well as the similarities and differences between these approaches and the CS. The formal CS solution will then be presented in Sec. III. This section has a brief calculation to illustrate the gain in efficiency of the CS over an explicit finite difference calculation and presents a useful near-steady-state approximation. Section IV will then step through the essentials of a simplified CS example in two dimensions. This model is presented for pedagogical purposes, but would also be a most realistic model of ion transport when charge exchange collisions dominate. This is followed by a detailed description of a more sophisticated CS implementation in three independent variables, a model appropriate for the electrons in the CF of a helium dc glow discharge. A swarm in uniform E/N and a CF calculation using fixed electric field configurations will then be presented and compared with Monte Carlo simulations and experimental results. Finally, a CF calculation with a self-consistent electric field will be presented and discussed in Sec. VI. Factors influencing the accuracy of the predicted electric field configuration will be discussed, along with some of the obstacles that must be overcome to allow a realistic negative glow (NG) model and a self-consistent electrode-to-electrode calculation.

II. RELATED SOLUTION TECHNIQUES

The "convective scheme" (CS) presented here, which is based on a propagator or Green's-function method, combines aspects of a variety of techniques which have been applied to the CF problem. Details of the techniques relevant to the CS, along with recent or notable illustra-

tive published work, will now be discussed.

Fluid equations have been used extensively to model the cathode fall.^{3,4} Three coupled differential equations are generated from the zero, first, and second velocity moments of Boltzmann's equation. No form of the distribution function is assumed; the first three moments of the distribution function are proportional to the number, momentum, and energy densities, respectively. However, fluid equations will not distinguish between various distribution functions as long as they have identical zero, first, and second moments. Fluid approaches can produce reasonable results, but errors associated with this approximation are difficult to estimate.

In a related approach which is computationally similar to fluid equations, a distribution function with n free parameters is assumed and substituted into Boltzmann's equation. The first n velocity moments of Boltzmann's equation are integrated to obtain n coupled differential equations.⁵ The authors used this technique to illustrate an overall method of tackling the CF.²

Segur and Keller⁶ have manipulated Boltzmann's equation into a purely integral form and solved a CF problem with an imposed electric field. The method involves finding a matrix of "probability coefficients" for every electric field of interest and yielded results consistent with Boeuf and Marode's Monte Carlo results in the case of isotropic scattering.^{7,8}

The method of explicit finite differences has been directly applied to Boltzmann's equation. The method has been used by Kitamori *et al.* to study relaxation properties of spatially invariant problems.⁹ Time evolution information is available, as the calculation is iterated in time until a steady-state solution is found. The method is numerically intensive because of a stringent limit on the time step, the Courant-Friedrichs-Lewy (CFL) criterion.¹⁰ The time step must be small enough that no particles in the calculation cross more than a single mesh in a time step Δt . The limit is numerical (depending upon the nature of the imposed numerical mesh) rather than physical (limited by some physical process), though the choice of mesh size was presumably based on physical grounds.

In principle, an explicit finite difference calculation could integrate the spatial coordinate z away from a point where the velocity distribution is known, rather than iterating in the time variable. This would reduce the number of variables in a CF calculation by one. Finding such a point is problematic, and any changes to the electric field (such as occur during iteration to a self-consistent field) would require a recalculation of the entire distribution function for all z . An implicit finite difference calculation would not be restricted by the CFL constraint, but such a scheme relies heavily on the efficiency of solving tridiagonal matrix equations. Unfortunately, the collisions in the kinetic problem imply that the matrices are *not* tridiagonal, and much of the computational efficiency is lost.

Hybrids of these methods have been used extensively. A common hybrid is the expansion of the angular part of the distribution function of l Legendre polynomials to obtain l coupled differential equations.^{11,12} The number of

independent variables in Boltzmann's equation is thereby reduced at the expense of increasing the number of equations.

Monte Carlo simulations have been used to describe the electron behavior in the CF.^{7,13,14} These simulations exactly track the kinetics of the sampled electrons, but self-consistent calculations demand good number density statistics at *all* spatial locations in the discharge. State-of-the-art Monte Carlo calculations⁷ track each individual electron avalanche until the electrons hit an electrode, so no information is available on the time evolution of the discharge, and any adjustments of the electric field require a complete recalculation of the distribution. However, where the steady-state solution is important and good electric field and cross-section data are available, Monte Carlo simulations can generate results in excellent agreement with experiment.¹⁵

The CS to be presented here produces a distribution function which is a solution of the appropriate kinetic equation.¹⁶ The CS is perhaps closest in spirit to particle-in-cell simulations, but no random numbers are needed. When the CS is used with small time steps, the CS is mathematically identical to the method of finite differences¹⁶ (specifically, a donor cell or "up-streaming" method). Its implementation is very physical and intuitive, similar to a Monte Carlo scheme. It is a fully kinetic solution and therefore free of the errors that hamper fluid calculations and approaches that involve the assumption of a parametrized form of the distribution function. Unlike explicit finite differences, CS time steps are not restricted by the Courant-Friedrichs-Lewy criterion, but rather by the nature of the collisions. Specifically, the CS time step must be less than the smallest collision time in the energy range of interest. As implemented, the CS assumes no particles have undergone more than one collision during a time step, so inaccuracy arises once a time step becomes a large fraction of an average collision time (and a non-negligible fraction of particles have in reality undergone more than one collision during the time step).

III. CONVECTIVE SCHEME

A general description of the CS method for systems of rate equations is given by Adams and Hitchon¹⁷ and for kinetic equations by Hitchon *et al.*¹⁶ The details of a particle mover for one space and one velocity variable are covered in Ref. 16. This paper will emphasize the generalizations necessary for a CF calculation—an additional velocity coordinate, a non-Cartesian phase space, a detailed treatment of the important electron-atom collision processes, and convergence to a self-consistent solution. This section outlines the formal CS solution, demonstrates the efficiency of the CS relative to finite difference calculations, and presents a near-steady-state approximation that simplifies scattering calculations.

A. Formal solution

Formally, the CS requires the determination of the fraction p of particles in a cell of phase space at $(\mathbf{r}'', \mathbf{v}'')$ that move to a new cell of phase space at $(\mathbf{r}', \mathbf{v}')$ after a

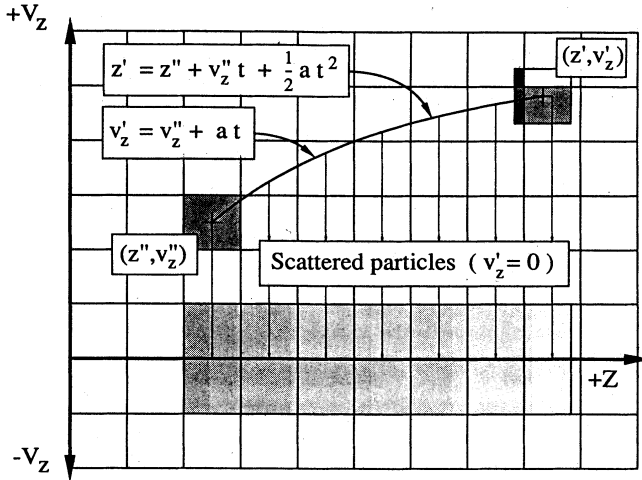


FIG. 1. Illustration of the ion convective scheme. Problem is one dimensional with two phase-space variables z and v_z . Force (electric field) is assumed constant. Scattering shown is analogous to resonant ion charge exchange; particles completely stop after a collision. Note that the mesh straddles the $v_z = 0$ axis to avoid possible singularities.

time Δt —the Green's function. (For consistency, doubly primed variables will always denote values *before* a movement or collision, and singly primed variables will label the values *after* the same.) Once this probability is known for all $(\mathbf{r}'', \mathbf{v}'')$ and $(\mathbf{r}', \mathbf{v}')$, the distribution of particles f at an advanced time $t + \Delta t$ may be determined given the distribution at time t ,

$$f(\mathbf{r}', \mathbf{v}', t + \Delta t) = \int d\mathbf{r}'' d\mathbf{v}'' p(\mathbf{r}', \mathbf{v}'; \mathbf{r}'', \mathbf{v}''; \Delta t) \times f(\mathbf{r}'', \mathbf{v}'', t). \quad (1)$$

When implemented on a numerical mesh, the integral becomes a sum over all cells of phase space in the mesh.

The task of evaluating p may seem daunting until it is realized that only two mechanisms can remove particles from a particular cell of phase space in the kinetic problem.

(i) Unscattered particles in a cell will move along characteristic trajectories specified by the initial position \mathbf{r}'' and velocity \mathbf{v}'' associated with the cell, the electric field \mathbf{E} along the trajectory, and the time step Δt .

(ii) Scattered particles will "jump" from the initial cell $(\mathbf{r}'', \mathbf{v}'')$ to a new cell at the same spatial location ($\mathbf{r}' = \mathbf{r}''$) but with a new velocity \mathbf{v}' defined by the nature of the collision.

These two processes are illustrated for a phase space with one spatial and one velocity coordinate in Fig. 1, which will be described in more detail in Sec. IV.

B. Time step

The two particle-moving mechanisms outlined in Sec. III A can be implemented independently of each other provided that the distribution function changes on a time scale much longer than the time step and provided that

no particle undergoes more than one collision per time step. The latter condition can be approximately enforced by limiting the time step Δt so that the fraction of particles that undergo two collisions in a time step is negligible,

$$[N\sigma_T(v)v\Delta t]^2 \ll 1 \quad (2)$$

for every speed v of interest. The left-hand side of Eq. (2) is proportional to the error of the CS, but the full CS error is further reduced to the extent that scattering into a cell replaces scattering out of the cell.

The advantage of the CS over its finite difference cousin can then be seen by examining Fig. 2. Here, the mean collision time is plotted versus impact energy for electrons in the background gas of interest here (helium) at a density of $N = 11.2 \times 10^{16} \text{ cm}^{-3}$. The important feature of Fig. 2 is that the collision time minimizes at some energy (here around 80 eV) and then generally increases with increasing impact energy. This minimum governs the allowable CS time step; here we choose a time step of $\Delta t \ll 0.12 \text{ ns}$ consistent with the energies of a normal helium CF (up to 140 eV) and the neutral number density of interest. This CS time step does not change, even if electrons of very high energy are considered.

Contrast this time step limit with the Courant-Friedrichs-Lewy (CFL) criterion¹⁰ that governs explicit finite difference methods: No particles may cross more than one cell in a time step. The limit applies to all independent variables in the problem; for a spatial variable x , even the fastest particles may not move more than the width of a single spatial cell Δx ,

$$\Delta t_{\text{CFL}} < \Delta x / v_{\text{max}}. \quad (3)$$

In a kinetic calculation, the spatial grid spacing is chosen to be at most the order of the minimum mean free path λ : $\Delta x < \langle \lambda \rangle = \langle N\sigma_T(v) \rangle^{-1} \approx 0.012 \text{ cm}$ in this case. The total scattering cross section is $\sigma_T(v)$. With a maximum speed of interest $v_{\text{max}} \approx 7.0 \times 10^8 \text{ cm/s}$, correspond-

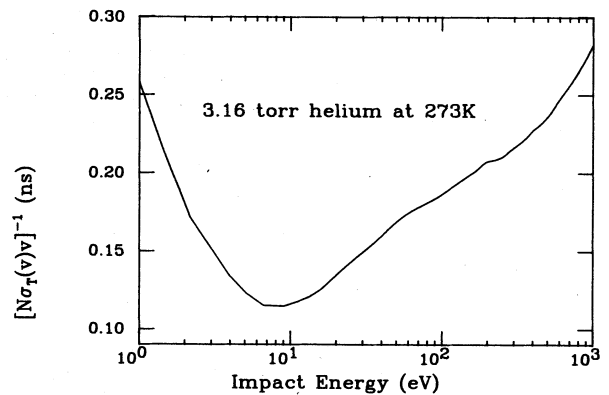


FIG. 2. Mean collision time for electrons in helium at $11.2 \times 10^{16} \text{ cm}^{-3}$ or 3.16 torr at 273 K. Minimum in the mean collision time within the energy range of interest governs the time step of the convective scheme.

ing to a normal CF potential energy in helium of around 140 V, the limiting time step from Eq. (3) is $\Delta t_{\text{CFL}} < 0.021$ ns. In practice, $\Delta t_{\text{CFL}} \ll 0.021$ ns unless a high-order scheme is used. Similar CFL limits exist for all other independent variables; for instance, the time step must also be limited to guarantee that no particles are accelerated through more than one cell in any velocity variable during Δt .

The advantage of the CS becomes even more apparent if electrons of higher energies are of interest, since $\Delta t_{\text{CFL}} \propto \tau_{\text{max}}^{-1/2}$, where τ_{max} is the maximum kinetic energy of interest, while the CS time step remains fixed.

C. Nearly-steady-state approximation

An initial examination of the scattering shown in Fig. 1 might seem to imply that the spatial movement of the particles in the initial cell must be considered when the particles scattered out of the cell during the time step are reinserted into the mesh. This might be true if the number of particles in a cell varied greatly over a time step.

This complication is not necessary here. In this work, particles scattered out of a cell initially at $(\mathbf{r}'', \mathbf{v}'')$ are replaced at $(\mathbf{r}' = \mathbf{r}'', \mathbf{v}')$ instead of being distributed along the same spatial trajectory that the initial cell traversed. The justification for this approximation rests upon the assumption that the number of particles at the initial location of the cell is roughly constant—particles may flow into and out of the cell during a time step, but in such a way as to approximately preserve the number of particles in the cell. The number of particles in a cell is certainly constant once a steady-state solution is obtained; provided the distribution changes on a time scale which is long compared to a time step, it is approximately true even during the transient solution. It would not be true, for example, if the CS were being used to study the expansion of a shock front, where particle densities vary greatly over a single spatial mesh cell and over a single time step.

IV. CONVECTIVE-SCHEME IMPLEMENTATION

A. Two-dimensional example

A simplified but complete CS model will now be examined. This model would be entirely reasonable for ions in their parent gas (dominated by charge exchange), but is simple enough to be described in one figure (Fig. 1). For simplicity, a uniform electric field is assumed. A few terms will be defined to clarify the description of the CS. The CS requires a numerical mesh; some of the considerations in choosing a mesh will be described. The focus of this section is to step through an entire iteration (time step) of the CS.

To avoid confusion, the following naming convention will be observed for cells.

(i) The *initial* cell will refer to the cell in which the particles are initially located (either at the beginning of a time step or just prior to a collision). The size and shape of the cell in the phase space mesh is part of the specification of the initial cell. Particles within a cell are assumed to be uniformly distributed within the cell; that is, the phase-space density of a cell is assumed constant.

As previously mentioned, initial variables will be doubly primed.

(ii) The *moved* cell will refer to the location, size, and shape of the cell, after either a ballistic particle movement or just after a collision. The size, shape, and density of the moved cell may differ from that of the initial cell depending upon the nature of the phase space, and the moved cell does not, in general, correspond to any single cell of the mesh. The phase-space density of the moved cell is also assumed constant. Variables associated with the moved cell will be singly primed.

(iii) The *final* cells are those cells of the mesh that are overlapped by the moved cell. For example, the moved cell may be larger than the initial cell or a final cell due to phase-space considerations. The larger moved cell could then overlap many final cells.

The first step of a CS solution is to choose an appropriate phase-space mesh that can accurately describe the important physical processes. The considerations are much the same as for a finite difference solution method. Ions in their parent gas are dominated by charge exchange collisions; such ions simply stop after an ion-neutral collision in the cold gas approximation (resonant charge exchange), and no energy is directed into the transverse direction. If plane-parallel geometry is assumed, two variables are sufficient for the ions—the distance from the anode z , and the ion velocity along the discharge axis v_z .

A CS calculation is started by placing particles into the mesh; how this is done depends on the problem of interest. If the physical source of new ions is assumed spatially uniform and the ions start from rest, then new ions would be placed in the mesh in the cells corresponding to $\pm \Delta v_z / 2$ and uniformly distributed in z . The number of ions injected is determined from the ionization rate and the CS time step.

The CS now determines the fate of the ions in the mesh after a single time step Δt . As previously indicated, all particles are first moved as though no collisions occur. Then all collision rates are calculated and the scattered particles are redistributed.

The collisionless particle movement is a straightforward step and is shown for the ion phase space and a uniform electric field directed in the positive z direction in Fig. 1. Each cell of the mesh is considered in turn. The location z'' , and velocity v_z'' associated with the initial cell, combined with the electric field $E(z)$, and the time step Δt , completely specify the location z' and velocity v_z' of the moved cell. The equations shown in Fig. 1 assume a constant electric field: E_0 , with an ion acceleration of $a = q_+ E_0 / m_+$, where q_+ is the ion charge and m_+ is the ion mass. The position of the moved cell after a time step Δt is calculated, and the particles from the initial cell are distributed to final cells in proportion to the overlap of the moved cell with each of the four final cells. Realistic field configurations require a numerical integration. Each initial cell is examined in turn until all particles have been moved to their final positions.

The charge exchange collisions of this example are particularly easy to handle in the CS. Each cell of the mesh is examined in turn; the number of particles in a particu-

lar cell and the velocity associated with the cell are known. When combined with the neutral number density, the cross section, and the CS time step, the number of particles scattered out of the cell of interest can be found. These particles are removed from the initial cell and added to the two cells that straddle the $v_z=0$ axis at the same spatial location (see Fig. 1). A nonzero background gas temperature could be handled by inserting the scattered ions with a Maxwellian velocity distribution. The scattering calculation is simplified by the fact that each cell of the mesh may be examined independently. Scattering rates are typically independent of spatial location and electric fields; in this case, the scattering probabilities can be calculated once for each velocity of interest on the mesh and then used for subsequent scattering calculations.

Once all cells of the mesh have been moved and then scattered, various moments of the distribution such as the number density and flux are calculated. If the calculation is self consistent, the electric field is recalculated. A new iteration is then started in this example by again injecting ions uniformly throughout the discharge in accordance with the assumed ionization rate.

B. Three-dimensional electron model

A CS model of the electrons in a helium discharge will now be described, building upon the simpler ion model. The physical assumptions here are the same as described in Ref. 2. Briefly, the discharge is assumed to be plane parallel with negligible radial diffusion and an electric field directed along the axis of the discharge: $\mathbf{E}=E\hat{z}$. The positive z axis points away from the cathode. This coordinate is reversed from that defined for the ions in Sec. IV A.

An adequate CS model of the electrons demands a realistic description of the angular scattering processes. An extra independent variable is therefore added to the model to describe motion transverse to the discharge axis. The independent variables are now the distance from the cathode z , the speed v , and μ , the cosine of the angle θ between the velocity vector and the z axis ($\mu = \cos\theta$). The discharge is azimuthally symmetric, so the azimuthal angle φ does not appear.

A mesh equally spaced in speed (rather than energy) is chosen for good resolution of the low-energy particles. To improve numerical accuracy, the mesh is finer near $\mu=1$ (forward-directed particles) than near $\mu=-1$ (backward-going particles). Specifically, a new integer variable ξ which labels cells is introduced which has limits $0 < \xi < \xi_{\max}$. Then μ at the boundary of the cells is calculated from $\mu = 1 - 2(\xi/\xi_{\max})^2$. The electric field moves unscattered particles monotonically to higher μ , and the use of the variable ξ improves the resolution in the region near $\mu=1$ in the mesh. (Note that this variation in mesh size is implemented with no difficulty, whereas the time step of a finite difference scheme would have to be reduced to accommodate the fine mesh near $\mu=1$ and again ensure that no particles could transverse more than one of these smaller cells in a time step. Additional coding difficulties would also arise. The CS mesh size can be varied at will to more accurately describe regions of in-

terest with no such ill effects.)

As with the ion example, the electron CS calculation is started by placing electrons in the mesh. Here electrons are placed in the cells of the mesh immediately adjacent to the cathode with an assumed distribution function so as to satisfy a current balance condition at the cathode. The details of this injection are not important to the CS; they will be discussed later as part of the self-consistent calculations.

1. Unscattered electrons

The ballistic movement of the electrons is more complex than that of the ions described previously. The complications arise out of the nature of the electron mesh, which has a variable Jacobian.

The ion CS model is considerably simplified by the fact that the ion phase space is Cartesian, and the size and shape of the cells do not change throughout the mesh. In general, the moved cell overlaps four final cells. The same cannot be said for the electron model; the Jacobian for this mesh is (approximately) $2\pi v^2$. A moved cell may fall completely within one final cell or may overlap many final cells. The CS accounts for this apparent variation in cell size by independently moving the center of each face of the initial cell to properly calculate the location and size of the moved cell. As before, the particles in the moved cell are distributed to each of the final cells in proportion to the volume of phase space occupied by the moved cell in each of the final cells.

2. Scattered electrons

The scattering calculations for the electrons are illustrated in Fig. 3, and described here. All scattering processes are assumed isotropic, with the anisotropic differential elastic cross section being replaced with the

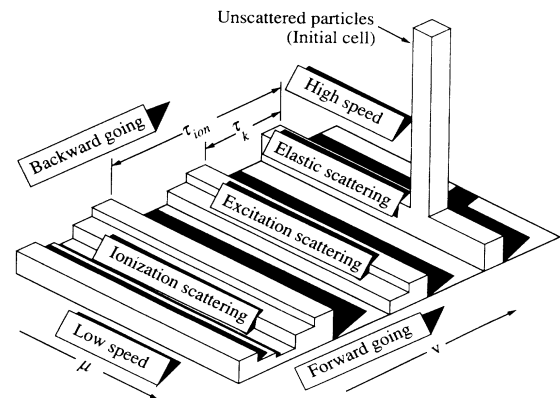


FIG. 3. Schematic of the electron collision operator. Electrons leaving a scattering event are distributed isotropically; anisotropic elastic scattering is described through the elastic momentum-transfer cross section. Electrons involved in an ionization event are distributed according to the differential energy scattering cross section. Ionization energy is τ_{ion} . Excitation energy for the single process shown is τ_k . Individual mesh cells have been omitted for clarity.

isotropic elastic momentum-transfer cross section. The assumption of isotropic inelastic scattering for electrons in a normal helium cathode fall is supported by the work of Den Hartog *et al.*¹⁵ A detailed investigation of the effects of anisotropic scattering in nitrogen is presented by Phelps and Pitchford.¹⁸ Although the present electron scattering calculations use isotropic scattering, it should be noted that any anisotropic distribution can be included in the CS.

The isotropic elastic momentum-transfer cross section is the simplest to examine. In this process, particles scatter from one polar angle μ'' to another μ' at the same speed ($v'=v''$). Particles scattered out within each cell (z'',v'',μ'') are replaced at the same spatial location z' and speed v' as the unscattered particles, but distributed evenly (isotropically) in the cosine of the polar angle μ' .

Excitation collision processes are similar, but the scattered particles are replaced isotropically at a final speed v' that is determined by the energy of the k th excitation process τ_k : $v'^2=v''^2-2\tau_k/m$. The phase space of the electron mesh compresses as one moves toward lower velocities. This is again handled by calculating the positions of the faces of the moved cell when scattering from one speed (v'') to another (v'); scattered particles lose a fixed energy τ_k , rather than a fixed speed.

Ionization processes produce scattered particles over a range of speeds $0 \leq v'^2 < v''^2 - 2\tau_{\text{ion}}/m$, where τ_{ion} is the ionization threshold energy. The number of particles scattered to each speed in this range is found using the differential energy ionization cross section. The scattered particles are then distributed isotropically as before.

As in the ion model, relevant moments of the distribution are calculated and (if self-consistent) the field is adjusted. As a final note, some moments are not found by integrating over the mesh. To improve the accuracy of finding moments like the average electron velocity $\langle v_z \rangle$ and the electron current density j_e , the electron flux across the z boundaries within the mesh is tracked during the unscattered movement of electrons and used to calculate $\langle v_z \rangle$ and j_e .

V. FIXED ELECTRIC FIELD CALCULATIONS

A. Swarm experiment calculations

The CS is now used to model a swarm experiment in helium at a uniform reduced field of $E/N=282$ Td (where $1 \text{ Td}=10^{-17} \text{ V cm}^2$). The gas density N is $3.53 \times 10^{16} \text{ cm}^{-3}$. The cross sections are taken from LaBahn and Callaway¹⁹ (elastic) and Alkhozov²⁰ (inelastic).

Figures 4(a)–4(d) show the predicted relative density n , the average z velocity $\langle v_z \rangle$, the average electron energy $\langle \tau \rangle$, and the effective Townsend first ionization coefficient α . The CS predictions are plotted, along with results from Doughty's Monte Carlo,²¹ which uses the full anisotropic elastic scattering cross section. The Monte Carlo simulation should otherwise be directly comparable to the predictions of the CS.

The exact nature of the equilibration region near the cathode depends upon assumptions made about the dis-

tribution of electrons liberated from the cathode surface. A perfectly absorbing anode is assumed in both calculations, producing the observed absence of backscattered electrons near the anode. Assumptions about the nature of the electrode boundaries are common to both the CS and Monte Carlo methods, but do not affect the predicted swarm values.

Results from swarm experiments of Küçükarpaci *et al.*²² are also displayed in Fig. 4. Küçükarpaci's results are in general agreement with an older but extensive set of swarm data compiled by Dutton.²³ Care has been taken to ensure a proper comparison of the average velocity $\langle v_z \rangle$ from the CS with the experimentally obtained drift velocity v_d . The average velocity attributed to Küçükarpaci in Fig. 4 was found using the drift velocity v_d , Townsend ionization coefficient α , and longitudinal diffusion D_L from Ref. 22,

$$\langle v_z \rangle = \frac{\Gamma}{n} = v_d - D_L \alpha. \quad (4)$$

The electron flux Γ and density n are well-defined moments.

The agreement of the predicted and experimental values is excellent. Küçükarpaci quotes an accuracy of $\pm 5\%$ in v_d and $\pm 15\%$ in D_L at this relative high E/N . The experimental uncertainties for α are larger; Dutton

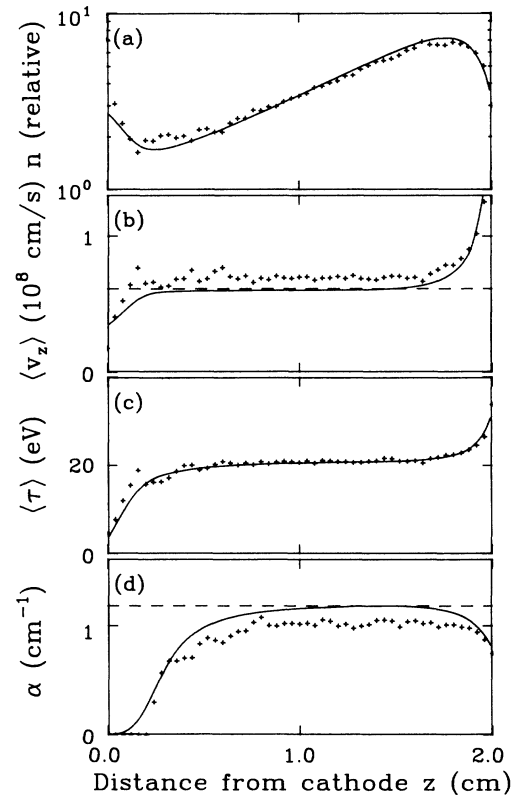


FIG. 4. Comparison of results of a swarm calculation. Solid lines denote the CS calculations and crosses are from the Monte Carlo calculation of Doughty (Ref. 21). Dashed lines indicate the experimental swarm values from Ref. 22 (see text).

discusses the problems in detail. The semiempirical inelastic cross sections from Alkhozov have an uncertainty of $\pm 25\%$ at low impact energies and $\pm 15\%$ at higher energies where the Born approximation is reliable. The differential elastic cross section from LaBahn and Callaway has an estimated accuracy of $\pm 5\%$.

B. Cathode fall

In this section the CS will be used to model the CF in the $j_D = 0.190 \text{ mA cm}^{-2}$ near-normal glow discharge of Doughty *et al.*²⁴ and Den Hartog *et al.*¹⁵

An electric field configuration is imposed based on the field experimentally measured using optogalvanic detection of Rydberg atoms.²⁵ A linear field is assumed in the CF based on a least-squares fit to experimental electric field data.^{15,24} The field is 897 V/cm at the cathode and extrapolates to zero at 0.382 cm from the cathode. The gas density is $11.2 \times 10^{16} \text{ cm}^{-3}$. A realistic model of the NG is beyond the scope of this paper, so a weak NG field was assumed (10 V/cm directed toward the cathode). This field configuration allows comparison with the Monte Carlo calculation, as the Monte Carlo calculation is unable to handle trapped particles (and therefore a field reversal). It also shortens the computation time required by sweeping electrons out of the NG region and into the anode.

A comparison of the results of the CS and Monte Carlo

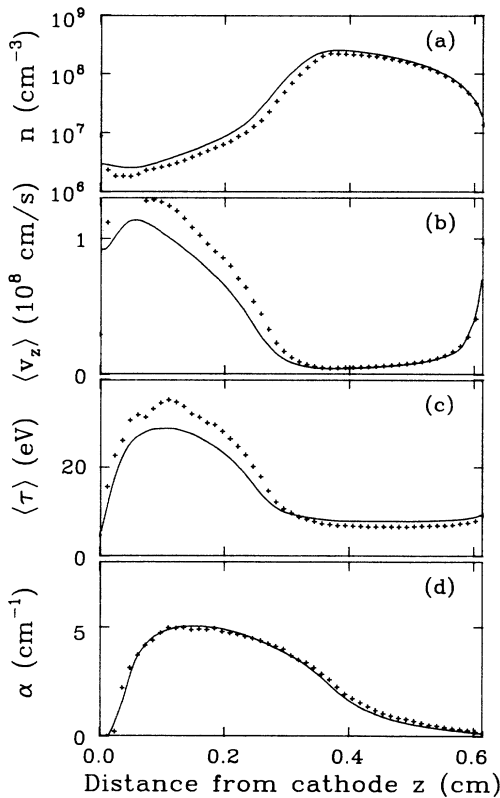


FIG. 5. Comparison of results for a near-normal glow discharge from the CS and Doughty's Monte Carlo calculations (Ref. 21). The parameters and imposed electric field correspond to the $j_D = 0.190 \text{ mA cm}^{-2}$ discharge of Ref. 24.

methods is shown in Fig. 5; the agreement here, as in the swarm calculations, is excellent. This fixed-field calculation should be an accurate indication of electron behavior in the CF. It should also be a reasonable model of the high-energy electrons that stream through the NG from the CF to the anode. It does not describe all of the NG electrons because the assumed NG field configuration does not allow a realistic anode sheath to form which would contain the highly mobile electrons within the NG plasma. A more detailed consideration of the NG will be presented along with the self-consistent CF calculations of Sec. VI C.

A brief review is in order. The CS method has been shown to accurately match the predictions of a fixed-field Monte Carlo code, where individual particle trajectories are followed exactly, unhampered by any mesh. Compared to an explicit finite difference solution, the CS algorithm is more efficient and free of numerical instabilities (it is inherently an integral, rather than a differential formulation). It is accurate *during* the time evolution of the system. Because the Green's function for the Boltzmann equation has an obvious interpretation, the CS method is very intuitive to implement, much in the spirit of Monte Carlo simulations.

VI. SELF-CONSISTENT ELECTRIC FIELD

A. Scope of solution

As mentioned in Sec. I, a self-consistent calculation of the CF demands an accurate description of all charged species. Here, singly charged ions (He^+) are assumed to be the only charged species present other than the electrons, and the ionic current is assumed to be the difference between the fixed discharge current and the electron current predicted by the CS [Eq. (6)]. Ion behavior is parametrized using the experimentally known mobility from Helm;²⁶ the details of this treatment and its justification in the CF are presented in Ref. 2.

Lawler²⁷ showed that the mobility parametrization of the ions should be adequate in the high-field part of the CF, but that the ion model is suspect near the CF-NG boundary. His calculations indicate that ions moving through rapidly changing fields (as exist near the CF-NG boundary) require several mean free paths to reach the speed indicated by the mobility, depending upon the actual field configuration and ionization source. The ion model does not describe the random thermal motion of the ions, which is important in low-field regions such as the NG. Because inertial effects are discounted, it cannot be expected to realistically model a possible field reversal in the discharge. The field must reverse somewhere in the discharge to allow the formation of an anode sheath and prevent a quick escape of NG electrons to the anode. Evidence placing the field reversal near the CF-NG boundary was recently reviewed by Den Hartog *et al.*¹⁵ Microwave Doppler-shift measurements have indicated a slow ion drift toward the anode in the NG of a Kr-D₂ glow discharge,²⁸ indicative of a weak reversed field in the NG.

The numerical problems associated with a field reversal are strictly a function of the crude ion transport model.

A field reversal could be handled with ease if the CS were also used to describe the ions.

A self-consistent model of the CF-NG boundary and the NG will not be considered in this paper for several reasons. The physical assumptions appropriate in the NG differ markedly from those of the CF. Several mechanisms have been discounted in the present CS model of the CF that may be important in the NG, including energy transfer during elastic collisions, a nonzero neutral gas temperature, electron-ion recombination, Coulomb collisions, and the role of metastable atoms. A discussion of these and other mechanisms in a helium afterglow can be found in a comprehensive paper by Deloche *et al.*²⁹

A more vexing problem is the physical time required to build up the large density of low-energy electrons existing in the NG. Recent experiments^{15,30} on the $j_D=0.190$ mA cm⁻² helium discharge being modeled here indicate a large density ($\geq 10^{11}$ cm⁻³) of relatively cold (≤ 0.25 eV) electrons in the NG. If this density extends over 0.1 cm (around half) of the NG, 10^{10} electrons would exist in the NG per square centimeter of electrode area. If the source of these electrons is taken to be the electronic current crossing from the CF into the NG ($j_e=j_D=0.190$ mA cm⁻² at the CF-NG boundary), and there are no losses (a best case assumption), it would take a minimum of 10^{-5} seconds for enough electrons to be generated in the discharge to obtain the observed NG electron density. Given the aforementioned CS time step of 0.05 ns (limited by the electron-atom collision rates in helium), this translates into a minimum of 2×10^5 CS iterations. A self-consistent electrode-to-electrode calculation must circumvent this problem.

B. Boundary condition at the cathode

While the absolute number density in a fixed-field solution may be scaled arbitrarily by varying the number of injected electrons, absolute number densities are required in a self-consistent calculation for use in Poisson's equation. As previously indicated, the driving source in the CF is the secondary emission of electrons from the cathode by ion, metastable, and uv photon impact. The appropriate number of electrons to be launched in the present model is found using an effective emission coefficient γ_p , which determines the ratio of electron current density j_e to ion current density j_{ion} at the cathode surface,

$$\gamma_p j_{ion}(0) = j_e(0). \quad (5)$$

As defined in Eq. (5), γ_p includes all emission mechanisms and a correction for electrons that are elastically backscattered to the cathode. The composite value of $\gamma_p \approx 0.3$ is taken from the experimental results of Doughty *et al.*²⁴ The determination of γ_p there is based on optogalvanic measurements of the electric field in a helium CF and the ion mobility as measured by Helm.²⁶

The ion current density at the cathode is found by fixing the discharge current density j_D throughout the discharge

$$j_D = j_{ion}(z) + j_e(z). \quad (6)$$

The electron current density at the cathode can be

found once the total current density j_D and the coefficient γ_p are specified. The CS is therefore started by placing electrons into the mesh cells adjacent to the cathode with a chosen velocity distribution so as to satisfy the conditions of Eqs. (5) and (6). The distribution of electrons ejected from the cathode is also assumed in Monte Carlo calculations; a flat energy distribution with energies of less than 10 eV is typical^{3,7,13,15,21,24} and reasonable in light of experimental measurements.³¹

C. Self-consistent calculations

The self-consistent problem demands an extra condition on the electric field to completely specify a unique solution. This condition is discussed in Ref. 2. Within the present model, the simple ion transport description requires the ion velocity, and hence the ion current, to vanish any time the electric field nears zero. The extremum condition of Ref. 2 should be useful for the more ambitious electrode-to-electrode calculation and a full investigation of the CF-NG boundary.

A self-consistent-field calculation is started by first guessing a field configuration [Fig. 6(a)] and then running a fixed-field calculation to (near) stability. In comparisons with Doughty, his CF field measurements were used as the initial guess. As in the fixed-field calculation, the

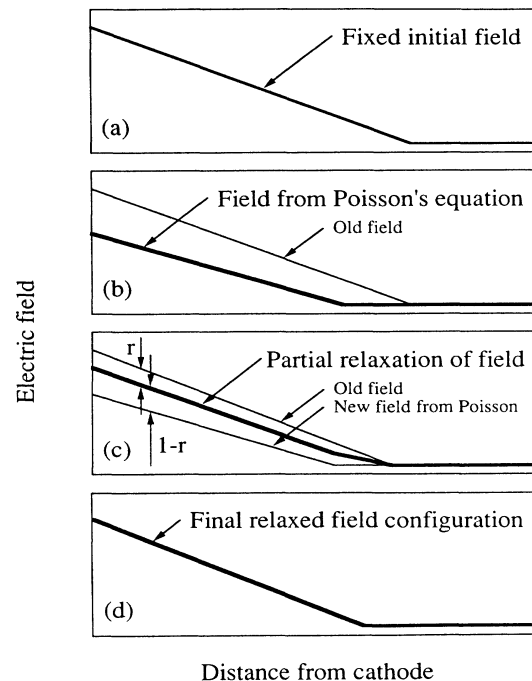


FIG. 6. Schematic of the field relaxation algorithm. Initial fixed-field configuration is guessed and the convective-scheme run to (near) stability (a). Poisson's equation is used to calculate a new field configuration (b). Old field is then allowed to relax a fraction r of the distance toward the new field (c). Partially relaxed field of (c) becomes the "old" field in (b) during the next iteration, and (b) and (c) are repeated until stability is again reached (d). Separation of the old and new fields, as well as the amount of relaxation r , have been exaggerated for clarity.

NG field is assumed to be directed toward the cathode with a magnitude of 10 V/cm, and the calculated field in the CF is matched to this value at the CF-NG boundary.

Once the fixed-field solution is found, Poisson's equation is combined with the field constraint ($j_{\text{ion}}=0$ if $E=0$) to calculate an electric field. A search is made for the spatial location where the electrons carry the full discharge current, that is, where $j_e=j_D$. This defines the CF-NG boundary. (Such a point may not exist if the guessed field is too weak; the initial guess must then be modified.) The calculated field is set to zero at this point and its behavior in the CF is found by integrating toward the cathode using Poisson's equation. The 10 V/cm NG field is then imposed throughout the NG. A typical result at this stage is shown in Fig. 6(b).

The field being used in the run (currently the imposed field) is allowed to relax a fixed fraction r (typically $r \approx 0.01$) of the difference between the field being used and the newly calculated field at each spatial location z [see Fig. 6(c)]. A single time iteration of the CS is calculated with the new field configuration, then the field is again relaxed. This scheme consisting of a single CS time iteration followed by a partial field relaxation is continued until a stationary solution is again found, as in Fig. 6(d).

VII. DISCUSSION OF SELF-CONSISTENT CALCULATION

The predicted electric field configuration for the $j_D=0.190 \text{ mA cm}^{-2}$ discharge of Doughty *et al.*²⁴ is presented in Fig. 7, along with the field measurements from optogalvanic experiments. The field decreases in a nearly linear fashion in the CF, as expected. The experimental and predicted fields are in good agreement in the high-field part of the CF. Factors influencing the predicted electric field will now be presented.

The slope of the predicted field in the CF is not directly dependent on the sophisticated kinetic treatment of the electrons; the electron density n is a negligible fraction of

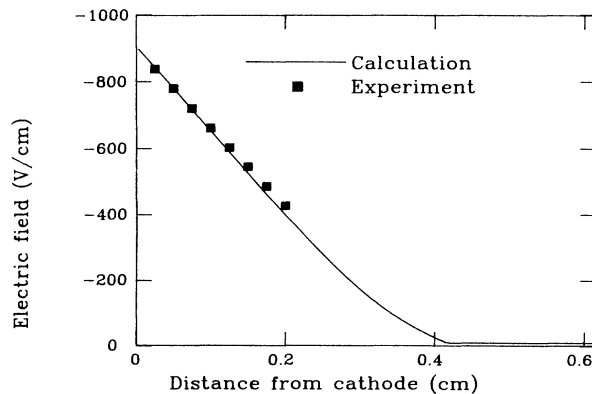


FIG. 7. Self-consistent electric field configuration as predicted by the convective scheme for the $j_D=0.190 \text{ mA cm}^{-2}$ discharge of Ref. 24. Experimental field points are optogalvanic measurements from the same reference.

the ion density n_+ , in the CF, so the ion density dictates the slope through Poisson's equation,

$$\frac{dE}{dz} = \frac{e}{\epsilon_0} n_+ . \quad (7)$$

The electric field is E , ϵ_0 is the permittivity of free space, and e is the unit charge ($e > 0$). Combining Poisson's equation with the current balance condition [Eq. (5)], continuity [Eq. (6)], and the mobility (μ_+) parametrization of the ion velocity v_+ ,

$$v_+ = \mu_+(E)E , \quad (8)$$

yields a constraint on the electric field at the cathode,

$$\mu_+(E)E \frac{dE}{dz} = \frac{j_D}{\epsilon_0(1+\gamma_p)} . \quad (9)$$

These considerations partially dictate the electric field configuration independent of the CS.

An accurate determination *has* been made of the electron current throughout the discharge, based on the de-

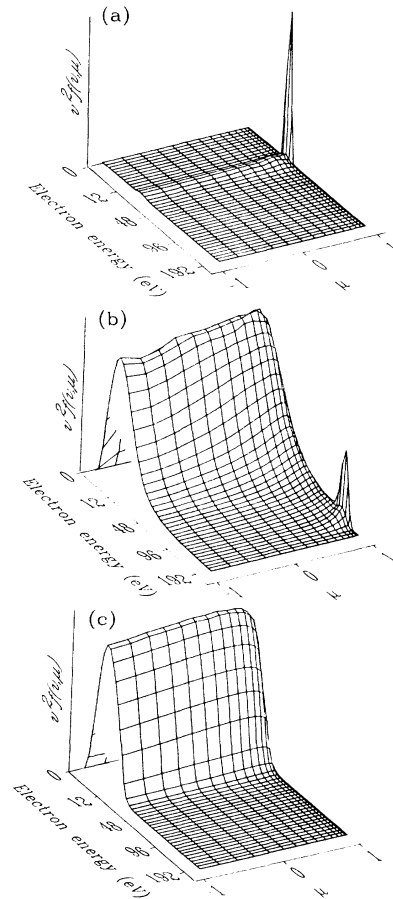


FIG. 8. Distribution functions from various spatial locations within the self-consistent CS calculation shown in Fig. 7. Distances from the cathode are (a) $z=0.028 \text{ cm}$ (near the cathode), (b) $z=0.243 \text{ cm}$ (midst of CF), and (c) $z=0.489 \text{ cm}$ (midst of NG).

tailed kinetic description of the CS. This, in turn, yields an accurate prediction of the ion current at all z through the continuity requirement [Eq. (6)]. The location of the CF-NG boundary is then fixed by requiring $j_e = j_D$ ($j_{\text{ion}} = 0$) at the boundary.

The calculated electronic current is dependent upon the absolute accuracy of the ionization rate. The ionization cross section is from Alkhozov,²⁰ and the uncertainties have already been discussed. Two simplifying assumptions in the CS also affect the ionization rate. Associative ionization is not included, and all electrons leave scattering events with isotropic distributions. The first assumption underestimates the total ionization; the second overestimates it because the isotropic assumption results in more backscattered high-energy electrons that are more likely to undergo additional ionization events. Anisotropic elastic scattering is already present in the Monte Carlo simulations, and some of the effects of anisotropic inelastic scattering can be included by assuming that the two electrons leaving an ionization event scatter elastically after the event with no recoil from the ionized atom.⁷ The Monte Carlo calculation indicates that the net result of these two assumptions is a slight underestimation of the ionization rate in the CS predictions in this near-normal discharge. An underestimation in the ionization rate corresponds to an overestimation of both the electric field strength in the CF and the length of the CF.

To emphasize the fully kinetic nature of this self-consistent calculation, distribution functions at three spatial locations in the discharge are presented in Fig. 8. Electrons that have survived unscattered from the cathode dominate Fig. 8(a), which is taken from near the cathode in the CF. Figure 8(b) is taken from the midst of

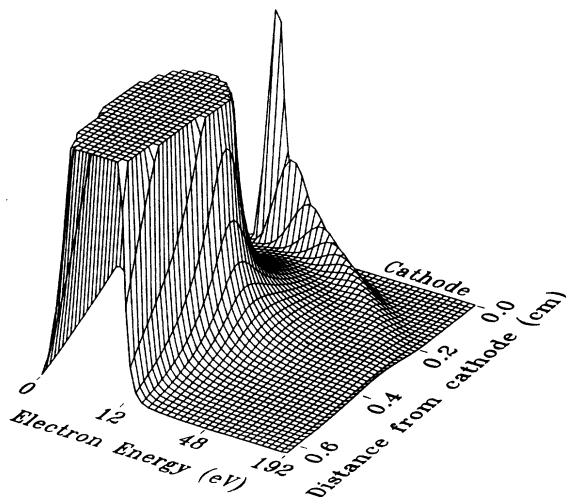


FIG. 9. Isotropic portion of the self-consistent electron distribution as a function of position within the discharge and electron speed. Vertical extent of the distribution function is truncated to show the unscattered beam of electrons from the cathode. Only every other mesh point in z is plotted for clarity.

the CF, showing the expected buildup of inelastically scattered electrons. Electrons streaming through the NG from the CF to the anode are shown in Fig. 8(c); this region is dominated by electrons that have undergone several inelastic collisions. The distribution differs somewhat from a pure Maxwellian—high-energy electrons are depleted relative to a Maxwellian due to inelastic collision processes, and close inspection of Fig. 8(c) reveals a slight anisotropy of the NG electrons. These electrons are sometimes called “beam” or “ballistic” electrons because they are distinctly nonhydrodynamic electrons in the weak NG electric field; they are primarily responsible for excitation and ionization events in the NG.

Finally, the isotropic part of the distribution function versus position in the discharge and electron speed is shown in Fig. 9. The vertical scale of the graph has been truncated at one-tenth the largest magnitude of the distribution function to more clearly show the beam electrons that have survived unscattered from the cathode.

VIII. SUMMARY

A convective-scheme method has been introduced to gaseous electronics in this paper. The method is more efficient than explicit finite difference schemes and able to accurately describe the time evolution of a plasma. The CS is very straightforward to implement, similar to Monte Carlo simulations. The CS was used to model two fixed-field discharges: a swarm experiment and the CF of a dc glow discharge. Predictions of the CS were shown to be consistent with Monte Carlo simulations. The swarm predictions were compared with experimental results, and uncertainties in both the experimental swarm results and the cross sections used in the CS were discussed. Self-consistent-field calculations of the CF were then presented. The field predicted by the self-consistent calculations was in excellent agreement with optogalvanic experiments. The accuracy of the electric field configuration was shown to depend on the detailed kinetic calculation primarily through the CS’s prediction of the electron current. This, in turn, fixed the location of the CF-NG boundary and yielded the predicted electric field configuration.

The problems hampering the present model near this boundary would be avoided with an improved ion transport model. Physical and numerical considerations necessary for a realistic model of the NG were outlined. The efficiency of the CS should eventually allow a fully kinetic treatment of both the electrons and ions and a complete electrode-to-electrode calculation, including a detailed description of the true nature of the CF-NG boundary.

ACKNOWLEDGMENTS

This research was supported by the U.S. Air Force Office of Scientific Research under Grant No. AFOSR 84-0328, the 3M Corporation, and the University of Wisconsin Engineering Research Center for Plasma Aided Manufacturing.

- ¹T. J. Moratz, L. C. Pitchford, and J. N. Bardsley, *J. Appl. Phys.* **61**, 2146 (1987).
- ²T. J. Sommerer, J. E. Lawler, and W. N. G. Hitchon, *J. Appl. Phys.* **64**, 1775 (1988).
- ³P. Bayle, J. Vacquie, and M. Bayle, *Phys. Rev. A* **34**, 360 (1986).
- ⁴J. P. Boeuf, *J. Appl. Phys.* **63**, 1342 (1988).
- ⁵John H. Ingold, in *Gaseous Electronics*, edited by M. N. Hirsh and H. J. Oskam (Academic, New York, 1978), Vol. I, Chap. 2, p. 37.
- ⁶Pierre Segur and Robert Keller, *J. Comput. Phys.* **24**, 43 (1977).
- ⁷J. P. Boeuf and E. Marode, *J. Phys. D* **15**, 2169 (1982).
- ⁸P. Segur, M. Yousfi, J. P. Boeuf, E. Marode, A. J. Davies, and J. G. Evans, in *Electrical Breakdown and Discharges in Gases*, Vol. 89A of *NATO Advanced Study Institute, Series B: Physics*, edited by E. E. Kunhardt and L. H. Luessen (Plenum, New York, 1983), p. 331.
- ⁹K. Kitamori, H. Tagashira, and Y. Sakai, *J. Phys. D* **11**, 283 (1978).
- ¹⁰R. Courant, K. Friedrichs, and H. Lewy, *Math. Ann.* **100**, 32 (1928).
- ¹¹L. C. Pitchford, in *Electrical Breakdown and Discharges in Gases*, Vol. 89A of *NATO Advanced Study Institute, Series B: Physics*, edited by E. E. Kunhardt and L. H. Luessen (Plenum, New York, 1983), p. 313.
- ¹²S. Yachi, Y. Kitamura, K. Kitamori, and H. Tagashira, *J. Phys. D* **21**, 914 (1988).
- ¹³Tran Ngoc An, E. Marode, and P. C. Johnson, *J. Phys. D* **10**, 2317 (1977).
- ¹⁴M. Ohuchi and T. Kubota, *J. Phys. D* **16**, 1705 (1983).
- ¹⁵E. A. Den Hartog, D. A. Doughty, and J. E. Lawler, *Phys. Rev. A* **38**, 2471 (1988).
- ¹⁶W. N. G. Hitchon, D. J. Koch, and J. B. Adams, *J. Comput. Phys.* (to be published).
- ¹⁷J. B. Adams and W. N. G. Hitchon, *J. Comput. Phys.* **76**, 159 (1988).
- ¹⁸A. V. Phelps and L. C. Pitchford, *Phys. Rev. A* **31**, 2932 (1985).
- ¹⁹R. W. LaBahn and J. Callaway, *Phys. Rev. A* **2**, 366 (1970); *Phys. Rev.* **180**, 91 (1969); *ibid.* **188**, 520 (1969).
- ²⁰G. D. Alkhazov, *Z. Tekh. Fiz.* **40**, 97 (1970) [*Sov. Phys.—Tech. Phys.* **15**, 66 (1970)].
- ²¹D. A. Doughty, Ph.D. thesis, University of Wisconsin, 1987.
- ²²H. N. Kükükarpaçi, H. T. Saelee, and J. Lucas, *J. Phys. D* **14**, 9 (1981).
- ²³J. Dutton, *J. Phys. Chem. Ref. Data* **4**, 577 (1975).
- ²⁴D. A. Doughty, E. A. Den Hartog, and J. E. Lawler, *Phys. Rev. Lett.* **58**, 2668 (1987).
- ²⁵D. K. Doughty and J. E. Lawler, *Appl. Phys. Lett.* **45**, 611 (1984).
- ²⁶H. Helm, *J. Phys. B* **10**, 3683 (1977).
- ²⁷J. E. Lawler, *Phys. Rev. A* **32**, 2977 (1985).
- ²⁸Hugh E. Warner, William T. Conner, and R. Claude Woods, *J. Chem. Phys.* **81**, 5413 (1984).
- ²⁹R. Deloche, P. Monchicourt, M. Cheret, and F. Lambert, *Phys. Rev. A* **13**, 1140 (1976).
- ³⁰E. A. Den Hartog, T. R. O'Brian, and J. E. Lawler, *Phys. Rev. Lett.* **62**, 1500 (1989).
- ³¹Homer D. Hagstrum, *Phys. Rev.* **104**, 672 (1956).